First study of η_{c}(1S), η(1760) and X(1835) production via η^{′}π^{+}π^{-} final states in two-photon collisions

C. C. Zhang *et al.* (The Belle Collaboration)

Phys. Rev. D **86**, 052002 — Published 10 September 2012

DOI: 10.1103/PhysRevD.86.052002

First study of $\eta_c(1S)$, $\eta(1760)$ and $X(1835)$ production via $\eta'\pi^+\pi^-$ final states in two-photon collisions

C. C. Zhang,[9] H. Aihara,[41] D. M. Asner,[32] T. Aushev,[12] A. M. Bakich,[37] Y. Ban,[33] K. Belous,[11] M. Bischofberger,[25] T. E. Browder,[6] A. Chen,[26] B. G. Cheon,[5] K. Chilikin,[12] R. Chistov,[12] Y. Choi,[36] J. Dalseno,[21,39] M. Danilov,[12] S. Eidelman,[1] M. Feindt,[15] V. Gaur,[38] N. Gabyshev,[1] Y. M. Goh,[5] Y. L. Han,[9] H. Hayashii,[25] Y. Horii,[24] W.-S. Hou,[27] H. J. Hyun,[18] T. Iijima,[24,23] K. Inami,[23] A. Ishikawa,[40] M. Iwabuchi,[45] T. Julius,[22] C. Kiesling,[21] H. O. Kim,[18] M. J. Kim,[18] Y. J. Kim,[16] B. R. Ko,[17] P. Kodyš,[2] S. Korpar,[20,13] P. Krokovny,[1] A. Kuzmin,[1] J. Li,[35] J. Libby,[8] Y. Liu,[3] Z. Q. Liu,[9] R. Louvot,[19] D. Matvienko,[1] S. McOnie,[37] R. Mizuk,[12] E. Nakano,[31] M. Nakao,[7] H. Nakazawa,[26] Z. Natkaniec,[28] S. Nishida,[7] T. Ohshima,[23] S. Okuno,[14] S. L. Olsen,[35,6] P. Pakhlov,[12] G. Pakhlova,[12] H. Park,[18] H. K. Park,[18] R. Pestotnik,[13] M. Petrič,[13] L. E. Piilonen,[44] M. Röhrken,[15] S. Ryu,[35] H. Sahoo,[6] Y. Sakai,[7] D. Santel,[3] T. Sanuki,[40] O. Schneider,[19] C. Schwanda,[10] M. E. Sevior,[22] M. Shapkin,[11] V. Shebalin,[1] C. P. Shen,[23] T.-A. Shibata,[42] J.-G. Shiu,[27] B. Shwartz,[1] P. Smerkol,[13] Y.-S. Sohn,[45] E. Solovieva,[12] S. Stanič,[30] M. Starič,[13] M. Sumihama,[4] T. Sumiyoshi,[43] I. Tikhomirov,[12] M. Uchida,[42] S. Uehara,[7] T. Uglov,[12] Y. Unno,[5] S. Uno,[7] G. Varner,[6] A. Vinokurova,[1] V. Vorobyev,[1] P. Wang,[9] X. L. Wang,[9] Y. Watanabe,[14] K. M. Williams,[44] B. D. Yabsley,[37] Y. Yamashita,[29] C. Z. Yuan,[9] Z. P. Zhang,[34] and V. Zhulanov[1]

(The Belle Collaboration)

[1] *Budker Institute of Nuclear Physics SB RAS and Novosibirsk State University, Novosibirsk 630090*
[2] *Faculty of Mathematics and Physics, Charles University, Prague*
[3] *University of Cincinnati, Cincinnati, Ohio 45221*
[4] *Gifu University, Gifu*
[5] *Hanyang University, Seoul*
[6] *University of Hawaii, Honolulu, Hawaii 96822*
[7] *High Energy Accelerator Research Organization (KEK), Tsukuba*
[8] *Indian Institute of Technology Madras, Madras*
[9] *Institute of High Energy Physics, Chinese Academy of Sciences, Beijing*
[10] *Institute of High Energy Physics, Vienna*
[11] *Institute of High Energy Physics, Protvino*
[12] *Institute for Theoretical and Experimental Physics, Moscow*
[13] *J. Stefan Institute, Ljubljana*
[14] *Kanagawa University, Yokohama*
[15] *Institut für Experimentelle Kernphysik, Karlsruher Institut für Technologie, Karlsruhe*
[16] *Korea Institute of Science and Technology Information, Daejeon*
[17] *Korea University, Seoul*
[18] *Kyungpook National University, Taegu*
[19] *École Polytechnique Fédérale de Lausanne (EPFL), Lausanne*
[20] *University of Maribor, Maribor*
[21] *Max-Planck-Institut für Physik, München*
[22] *University of Melbourne, School of Physics, Victoria 3010*
[23] *Graduate School of Science, Nagoya University, Nagoya*
[24] *Kobayashi-Maskawa Institute, Nagoya University, Nagoya*
[25] *Nara Women's University, Nara*
[26] *National Central University, Chung-li*
[27] *Department of Physics, National Taiwan University, Taipei*
[28] *H. Niewodniczanski Institute of Nuclear Physics, Krakow*
[29] *Nippon Dental University, Niigata*
[30] *University of Nova Gorica, Nova Gorica*
[31] *Osaka City University, Osaka*
[32] *Pacific Northwest National Laboratory, Richland, Washington 99352*
[33] *Peking University, Beijing*
[34] *University of Science and Technology of China, Hefei*
[35] *Seoul National University, Seoul*
[36] *Sungkyunkwan University, Suwon*
[37] *School of Physics, University of Sydney, NSW 2006*
[38] *Tata Institute of Fundamental Research, Mumbai*
[39] *Excellence Cluster Universe, Technische Universität München, Garching*
[40] *Tohoku University, Sendai*
[41] *Department of Physics, University of Tokyo, Tokyo*
[42] *Tokyo Institute of Technology, Tokyo*
[43] *Tokyo Metropolitan University, Tokyo*

[44] CNP, Virginia Polytechnic Institute and State University, Blacksburg, Virginia 24061
[45] Yonsei University, Seoul

The invariant mass spectrum of the $\eta'\pi^+\pi^-$ final state produced in two-photon collisions is obtained using a 673 fb^{-1} data sample collected in the vicinity of the $\Upsilon(4S)$ resonance with the Belle detector at the KEKB asymmetric-energy e^+e^- collider. We observe a clear signal of the $\eta_c(1S)$ and measure its mass and width to be $M(\eta_c(1S)) = (2982.7 \pm 1.8(stat) \pm 2.2(syst) \pm 0.3(model))$ MeV/c^2 and $\Gamma(\eta_c(1S)) = (37.8^{+5.8}_{-5.3}(stat) \pm 2.8(syst) \pm 1.4(model))$ MeV/c^2. The third error is an uncertainty due to possible interference between the $\eta_c(1S)$ and a non-resonant component. We also report the first evidence for $\eta(1760)$ decay to $\eta'\pi^+\pi^-$; we find two solutions for its parameters, depending on the inclusion or not of the $X(1835)$, whose existence is of marginal significance in our data. From a fit to the mass spectrum using coherent $X(1835)$ and $\eta(1760)$ resonant amplitudes, we set a 90% confidence level upper limit on the product $\Gamma_{\gamma\gamma}\mathcal{B}(\eta'\pi^+\pi^-)$ for the $X(1835)$.

PACS numbers: 13.25.Gv, 14.40.Gx, 13.66Bc, 12.38.Qk

I. INTRODUCTION

As the lowest charmonium state, the $\eta_c(1S)$ meson plays an important role in tests of QCD. However, even its main parameters, such as the mass, width and two-photon width, have not been well measured and the measurements that have been reported show a large scatter of values [1]. Discrepancies among measurements for the $\eta_c(1S)$ product of the two-photon width and decay branching fraction into four-meson final states were confirmed earlier [2]. A recent measurement of the $\eta_c(1S)$ that found a significant interference between the $\eta_c(1S)$ and the non-resonant background [3] may have clarified the reason for discrepancies among $\eta_c(1S)$ parameter measurements [4]. Significant model-dependent uncertainty in the measurement of the $\eta_c(1S)$ product branching fractions due to interference between the $\eta_c(1S)$ and a non-resonant component has also been studied in $B \to K\eta_c(1S)$ decays [5].

The $X(1835)$ resonance was observed and confirmed recently by the BES collaboration in $J/\psi \to \gamma X(1835)$ decays where $X(1835) \to \eta'\pi^+\pi^-$ [6], with mass $M = (1836.5 \pm 3.0^{+5.6}_{-2.1})$ MeV/c^2 and width $\Gamma = (190 \pm 9^{+38}_{-36})$ MeV/c^2. A variety of speculations on the nature of the $X(1835)$ have been reported, including baryonium [7] with sizable gluon content [8], glueball [9–11], and a radial excitation of the η' [12, 13]. The BES experiment has suggested that the $X(1835)$ may be related to the $p\overline{p}$ threshold enhancement seen in $J/\psi \to \gamma p\overline{p}$ decays [14, 15]. An additional structure, the $\eta(1760)$, was observed in the radiative J/ψ decays to $\gamma\rho\rho$ and $\gamma\omega\omega$ by MARKIII [16] and DM2 [17] and to $\gamma\omega\omega$ and $\gamma\eta\pi^+\pi^-$ by BES [18]. The $\eta(1760)$ state has been proposed as a mixture of a gluonic meson with a conventional $q\bar{q}$ state [19], rather than a pure $q\overline{q}$ meson, and this hypothesis is supported by a BES analysis of $J/\psi \to \gamma\omega\omega$ decays [18]. Hence, an investigation of the nature of both the $X(1835)$ and $\eta(1760)$ is of interest [20]. In radiative J/ψ decays, hadrons are produced via two gluons; thus, the production of final states with a gluon-enriched component is expected to be enhanced. In light of the similar structure of the two-photon and two-gluon couplings, a comparison of the $\gamma\gamma$ width of a meson to its production rate in radiative J/ψ decays can provide information on its quark and gluon composition. The two-photon coupling to the gluonic component is expected to be very weak so measurements of two-photon widths can help clarify the nature of the $X(1835)$ and $\eta(1760)$.

In this paper, we report the first observation of $\eta'\pi^+\pi^-$ production in two-photon collisions using a 673 fb^{-1} data sample (605 fb^{-1} on the $\Upsilon(4S)$ resonance and 68 fb^{-1} at 60 MeV below the resonance) accumulated with the Belle detector [21] at the KEKB asymmetric-energy e^+e^- collider [22]. We measure parameters of the $\eta_c(1S)$, provide first evidence for $\eta(1760) \to \eta'\pi^+\pi^-$ decay, and give limits on the two-photon production of the $X(1835)$.

II. DETECTOR AND MONTE CARLO SIMULATION

The Belle detector is a large-solid-angle magnetic spectrometer that consists of a silicon vertex detector, a 50-layer central drift chamber (CDC), an array of aerogel threshold Cherenkov counters (ACC), a barrel-like arrangement of time-of-flight scintillation counters (TOF), and an electromagnetic calorimeter comprised of CsI (Tl) crystals (ECL). These detectors are located inside a superconducting solenoid coil that provides a 1.5 T magnetic field. An iron flux return located outside the coil is instrumented to detect K^0_L mesons and to identify muons [21].

Monte Carlo (MC) events of the two-photon process $\gamma^*\gamma^* \to \eta'\pi^+\pi^-$ are generated with the TREPS code [23] based on an Equivalent Photon Approximation (EPA) [24], where the η' decays generically according to the JETSET7.3 decay table [25]. An isotropic phase space distribution is assumed for $\eta_c(1S)$, $\eta(1760)$ and $X(1835)$ decays to the three-body $\eta'\pi^+\pi^-$ final state. The GEANT-based simulation package [26] with trigger conditions included is employed for the propagation of the generated particles through the Belle detector.

III. EVENT SELECTION

The $\eta_c(1S)$, $\eta(1760)$ and $X(1835)$ (collectively denoted as R) candidates are reconstructed from the decay chain $R \to \eta'\pi^+\pi^-$, $\eta' \to \eta\pi^+\pi^-$, and $\eta \to \gamma\gamma$. Two photons and two $\pi^+\pi^-$ pairs are detected in the final state.

At least two neutral clusters and four charged tracks with zero net charge are required in each event. Candidate photons are neutral clusters that have an energy deposit greater than 100 MeV in the ECL and are not near any of the charged tracks. The polar angle of the charged tracks, *i.e.*, the angle with respect to the direction opposite the positron beam axis in the laboratory system, must satisfy $\cos\theta \in [-0.8660, +0.9563]$. To enhance the detection efficiency for low momentum charged tracks, loose requirements on the impact parameters perpendicular to (dr) and along (dz) the beam line from the interaction point are applied: $dr < 5$ ($< 3, < 2, < 1$) cm and $|dz| < 5$ ($< 5, < 4, < 3$) cm for the track transverse momentum $p_t < 0.2$ ($\in [0.2, 0.3], \in [0.3, 0.4], > 0.4$) GeV/$c$. The scalar sum of the absolute momenta for all the charged tracks and neutral clusters and the sum of the ECL cluster energies in the laboratory system are required to be $p_{\rm sum} < 5.0$ (< 5.5) GeV/c for the $\eta'\pi^+\pi^-$ system in the mass region below 2.7 GeV/c^2 (in the $\eta_c(1S)$ region) and $E_{\rm sum} < 4.5$ GeV.

Events with an identified kaon ($K^\pm$ or $K^0_S \to \pi^+\pi^-$) or proton are vetoed. For charged tracks, information from the ACC, TOF and CDC is combined to form a likelihood $\mathcal{L}$ for hadron identification. A charged track with the likelihood ratio of $\mathcal{L}_K/(\mathcal{L}_\pi + \mathcal{L}_K) > 0.8$ is identified as a kaon; one with $\mathcal{L}_\pi/(\mathcal{L}_\pi + \mathcal{L}_K) > 0.2$ as a pion. With these loose requirements, the efficiency for pion identification is about 99%. A proton is identified by the requirement $\mathcal{L}_p/(\mathcal{L}_p + \mathcal{L}_K) > 0.95$. K^0_S candidates are reconstructed from a pair of charged pion tracks with invariant mass within 16 MeV/c^2 (3σ) of the nominal K^0_S mass.

The η from $\eta' \to \eta\pi^+\pi^-$ decay is reconstructed via its two-photon decay mode, where the two-photon invariant mass is in the window $M_{\gamma\gamma} \in [0.524, 0.572]$ GeV/c^2 ($\pm 2\sigma$ of the nominal η mass). To suppress background photons from π^0 decay, we exclude any photon that, in combination with another photon in the event, has an invariant mass within the window $|M_{\gamma\gamma} - m_{\pi^0}| < 18$ MeV/c^2. The two-photon-energy asymmetry, $A_{\rm sym} = |E_{\gamma 1} - E_{\gamma 2}|/(E_{\gamma 1} + E_{\gamma 2})$, is required to be less than 0.8 to suppress the fake η combinatorial background. The η' candidate is reconstructed from the η candidate and the $\pi^+\pi^-$ track pair that results in an invariant mass within $M_{\eta\pi^+\pi^-} \in [0.951, 0.963]$ GeV/c^2 ($\pm 2\sigma$ of the nominal η' mass). To improve the momentum resolution of the η and η', a mass-constrained fit to the η and two separate fits to the η' (one with a constrained vertex and the other with the mass constrained to the η') are applied.

The $\eta'\pi^+\pi^-$ candidates are reconstructed by combining the η' candidate and the remaining $\pi^+\pi^-$ track pair. For multi-candidate events, the candidate with the smallest χ^2_m from the η' mass-constrained fit is selected. For $\eta'\pi^+\pi^-$ combinations with invariant mass $W = 1.84$ (2.98) GeV/c^2, 19% (7.1%) of the signal MC events have more than one candidate per event, from which the correct candidate is selected 98% (91%) of the time.

IV. BACKGROUND AND ITS FURTHER REDUCTION

Signal and non-resonant events can be produced in two-photon collisions via the processes $e^+e^- \to e^+e^-R$ and $e^+e^- \to e^+e^-\eta'\pi^+\pi^-$, respectively, where quasi-real photons are emitted from the beam e^+ and e^- particles at small angles with respect to the beam line. These events tend to carry small transverse momentum $|\sum \vec{p}^{\,*}_t|$, which is determined by taking the absolute value of the vector sum of the transverse momenta of η' and the $\pi^+\pi^-$ tracks in the e^+e^- center-of-mass system.

The η'-sideband, denoted η'-*sdb*, arises from $\eta\pi^+\pi^-\pi^+\pi^-$ and $\gamma\gamma\pi^+\pi^-\pi^+\pi^-$ (without η) combinations that survive the η' selection criteria except that the $\eta\pi^+\pi^-$ combination whose mass is nearest that of the η' lies between 0.914 and 0.934 GeV/c^2 or between 0.98 and 1.0 GeV/c^2. Similar events with an $\eta\pi\pi$ mass within the η' acceptance window form a featureless background denoted b_1 in the R-candidate sample. The $\eta'\pi^+\pi^-X$ background, denoted b_2, has additional particles in the event beyond the R candidate. Other non-exclusive backgrounds, including those arising from initial state radiation, are found to be negligible.

A. Optimization for $|\sum \vec{p}^{\,*}_t|$ requirement

Significant background reduction is achieved by applying a $|\sum \vec{p}^{\,*}_t|$ requirement. The $|\sum \vec{p}^{\,*}_t|$ distribution for the signal peaks at small values, while that for both backgrounds decreases toward $|\sum \vec{p}^{\,*}_t| = 0$ due to vanishing phase space [27].

The $\eta_c(1S)$ state is well established [2, 6, 28] and its signal yield in our data sample is large. We utilize a control sample of $\eta'\pi^+\pi^-$ candidates from half the data, with W between 2.6 and 3.4 GeV/c^2, to establish the $|\sum \vec{p}^{\,*}_t|$ requirement under the assumption that the $|\sum \vec{p}^{\,*}_t|$ distribution is similar for events with $W < 2.2$ GeV/c^2. The

η'-*sdb* events from the full data sample are added to this control sample under the assumption that their $|\sum \vec{p}_t^{\,*}|$ distribution is similar to that of the b_1 background so that the signal fraction in this control sample is close to that in the W mass region below 2.2 GeV/c^2 in the full data sample. We use the relative statistical error for the $\eta_c(1S)$ yield in fitting the $\eta'\pi^+\pi^-$ mass spectra to optimize the $|\sum \vec{p}_t^{\,*}|$ requirement. The requirement $|\sum \vec{p}_t^{\,*}| < 0.09$ GeV/c (p_t-balanced) is applied to the R-candidate sample since it minimizes this relative error.

B. Background estimation

The b_1 component in the $\eta'\pi^+\pi^-$ mass and $|\sum \vec{p}_t^{\,*}|$ distributions are determined in the fits to the η'-*sdb* events (normalized) in the p_t-balanced and p_t-unbalanced (see below) samples, respectively. The residual b_2 component in the final R-candidate sample can be separated using the $|\sum \vec{p}_t^{\,*}|$ distribution. By doing so, its distribution in $\eta'\pi^+\pi^-$ mass is determined. Figure 1 shows the $|\sum \vec{p}_t^{\,*}|$ distribution for signal MC events and data in the mass region below 2.2 GeV/c^2.

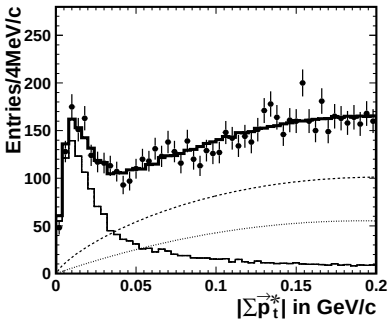

FIG. 1: The $|\sum \vec{p}_t^{\,*}|$ distributions for the mass region below 2.2 GeV/c^2 the data sample. The data points with error bars are from the $\eta'\pi^+\pi^-$-candidate sample before the $|\sum \vec{p}_t^{\,*}|$ requirement, the thick-solid histogram is the best fit, the thin solid histogram is the signal component, the thin-dashed curve is the b_1 component (whose shape is taken from the η'-*sdb* sample), and the thin-dotted curve is the b_2 component.

A p_t-unbalanced data subsample, in which the backgrounds dominate over the signal, is selected with the requirement $|\sum \vec{p}_t^{\,*}| \in [0.15, 0.2]$ GeV/c. The $\eta'\pi\pi$ mass distribution of this p_t-unbalanced subsample is fit to two separate background functions, one for the b_1 component with its yield and shape fixed at the values determined using the corresponding η'-*sdb* sample and the other for the b_2 component with its yield y_{unbal} and shape parameters allowed to float. We use the same shape for the b_2 component in the later fit to the $\eta'\pi^+\pi^-$ mass spectrum for the final R-candidate sample. Here, the assumption of the same shape in the invariant mass distribution for the b_2 component in the p_t-balanced and -unbalanced samples is implied. In the fit shown in Fig. 1, the signal function for R and non-resonant events is defined by a histogram of the signal MC events with its shape parameters fixed but yield floated; the b_1 component is described by a threshold function with its yield and shape parameters fixed; the b_2 component is described by a quadratic function with its yield and shape parameters floated. Here, the quadratic function for the b_2 is constrained to the origin, since b_2 background events selected as $\eta'\pi^+\pi^-$ with missing X should have non-zero transverse momentum. From the fit, we obtain the b_2 yields in the p_t-balanced and -unbalanced subsamples; the ratio of these yields is $y_{bal}/y_{unbal} = 0.723 \pm 0.043$. (The corresponding b_2 yield ratio for $2.6\,\mathrm{GeV}/c^2 < W < 3.4\,\mathrm{GeV}/c^2$ is 0.93 ± 0.11.) The b_2 yield y'_{bal} in the $\eta'\pi^+\pi^-$ mass spectrum for the final R-candidate sample is obtained from the yield y'_{unbal} scaled to this ratio.

The invariant mass distributions for the $\eta'\pi^+\pi^-$ candidates, as well as those for the b_1 and b_2 backgrounds, are shown in Fig. 2. In addition to the prominent $\eta_c(1S)$ signal, an enhanced shoulder is evident in the mass region below 2 GeV/c^2 in the b_1- and b_2-subtracted histogram of Fig. 2(b). The robust enhancement is also seen in the $\eta'\pi^+\pi^-$ yields extracted from fitting the $|\sum \vec{p}_t^{\,*}|$ distributions in each sliced mass bin, shown as data points with error bars in Fig. 2(b).

V. FITTING MASS SPECTRUM

The cross section of R production in the two-photon process $e^+e^- \to e^+e^-R$ is approximated by

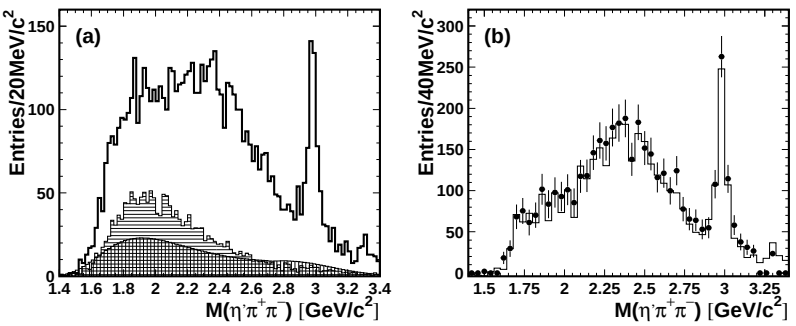

FIG. 2: Invariant mass distribution for the $\eta'\pi^+\pi^-$ candidates. (a) The open histogram represents the data; the horizontal (vertically) hatched histogram is the contribution from the b_1 (b_2) background. (b) The histogram shows the data after subtraction of both the b_1 and b_2 background components; the points with error bars are the $\eta'\pi^+\pi^-$ yields extracted from fitting the $|\sum \vec{p}_t^{\,*}|$ distribution in each sliced mass bin.

$$\sigma(e^+e^- \to e^+e^- R) \;=\; \int \sigma_{\gamma\gamma\to R}(W)\frac{dL_{\gamma\gamma}}{dW}dW, \tag{1}$$

where the two-photon luminosity function $\frac{dL_{\gamma\gamma}}{dW}$ is calculated in the EPA using TREPS and the cross section $\sigma_{\gamma\gamma\to R}(W)$ for C-even resonance production with zero spin is described by a Breit-Wigner (BW) function $f_{BW}(W)$ [24]:

$$\sigma_{\gamma\gamma\to R}(W) = f_{BW}(W)\cdot\Gamma_{\gamma\gamma} = \frac{8\pi\Gamma\cdot\Gamma_{\gamma\gamma}}{(W^2-M^2)^2+\Gamma^2M^2}, \tag{2}$$

where M, Γ and $\Gamma_{\gamma\gamma}$ are the mass, total width and two-photon decay width of the R, respectively.

The signal yield n_s, M and Γ are extracted by maximizing the extended likelihood function,

$$\mathcal{L} = \frac{e^{-(n_s+\sum_{k=1}^{3} n_{b,k})}}{N!}\prod_{i=1}^{N}[n_s\cdot f_s(u_i;M,\Gamma)+\sum_{k=1}^{3} n_{b,k}\cdot f_{b,k}(u_i;p_{b,k})], \tag{3}$$

where n_s ($n_{b,k}$) is the number of signal (k-th background component) events, N is the total number of candidate events, i is the event identifier and u_i is the measured invariant mass for the i-th event. The probability density function (PDF) f_s for the R signal is a BW function convolved with mass resolution after corrections for $\frac{dL_{\gamma\gamma}}{dW}$ and the efficiency. The k-th background's PDF and its parameters are denoted by $f_{b,k}$ and $p_{b,k}$, respectively. In the fit, n_s, M and Γ for the signal are allowed to float unless stated otherwise; $n_{b,k}$ and $p_{b,k}$ for non-resonant background (NR) are allowed to float while those for the b_1 and b_2 backgrounds are fixed. Two distinct fits are performed: in the lower mass region $1.4\,\mathrm{GeV}/c^2 < W < 2.7\,\mathrm{GeV}/c^2$ where the NR (as well as b_1 and b_2) background component is described by a threshold function [29] with a reasonable description of the threshold effect, and in the higher mass region $2.6\,\mathrm{GeV}/c^2 < W < 3.4\,\mathrm{GeV}/c^2$ (near the $\eta_c(1S)$) where all the background components are described by an exponential of a third-order polynomial.

The evaluation of the significance of any marginal R signal in the lower-mass fit is sensitive to the assumed background shape. We have examined results of various fits with different descriptions of the background: (1) one threshold function for a sum of all three background components (*i.e.*, b_1, b_2 and NR); (2) two separate threshold functions, one for b_1 and the other for b_2 plus NR; (3) three separate threshold functions, one each for b_1, b_2 and NR, respectively; (4-6) the three background functions defined above, in each case convolved with a mass resolution function after corrections for the two-photon luminosity and efficiency. We fit the $\eta'\pi^+\pi^-$ mass spectrum for a possible $\eta(1760)$ signal in the mass region below 2.7 GeV/c^2 using the six different background models described above. Option (3) provides the smallest statistical significance for a signal resonance, and is conservatively chosen for the background description.

The product of the two-photon decay width and the $\eta'\pi^+\pi^-$ branching fraction for the R is determined as:

$$\Gamma_{\gamma\gamma}\mathcal{B}(R\to\eta'\pi^+\pi^-) = \frac{n_s}{L_{int}\cdot\int f_{BW}(W)\frac{dL_{\gamma\gamma}(W)}{dW}\epsilon(W)dW}, \tag{4}$$

where the efficiency ϵ includes the branching fractions for $\mathcal{B}(\eta'\to\eta\pi^+\pi^-)$ and $\mathcal{B}(\eta\to\gamma\gamma)$.

A. Results of the $\eta(1760)$ fit

We assume that only one resonance is produced in the mass range below 2.7 GeV/c^2 and that there is no interference between the signal and NR components. Figure 3 shows the results of the fit for the decay $R \to \eta'\pi^+\pi^-$. A signal with a yield $n_s = 465^{+131}_{-124}$ and a statistical significance of 4.8σ is found with mass $M = (1768^{+24}_{-25})$ MeV/c^2 and width $\Gamma = (224^{+62}_{-56})$ MeV/c^2; we denote this as $\eta(1760)$. The statistical significance, in units of standard deviation (σ), is calculated using the χ^2 distribution $-2 \cdot \ln(\mathcal{L}_0/\mathcal{L}_{max})$ with $N_{\rm dof}$ degrees of freedom. Here, $\mathcal{L}_{max}$ and $\mathcal{L}_0$ denote the maximum likelihood with the signal yield floating and fixed at zero, respectively, and $N_{\rm dof} = 3$ is the difference in the number of floating parameters between the nominal fit and the fit with the signal yield fixed at zero. The product of the two-photon decay width and branching fraction is determined to be $\Gamma_{\gamma\gamma}\mathcal{B}(\eta(1760) \to \eta'\pi^+\pi^-) = (28.2^{+7.9}_{-7.5})$ eV/c^2.

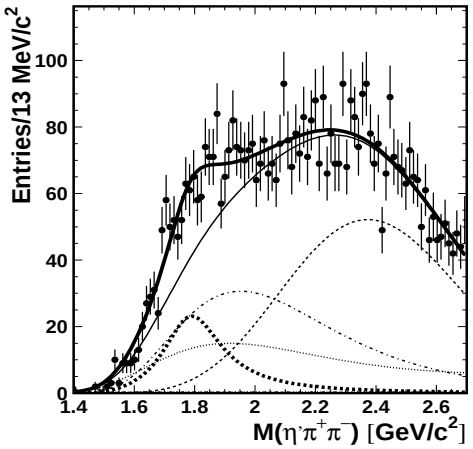

FIG. 3: The invariant mass distribution for $\eta'\pi^+\pi^-$ candidates in the lower-mass region. The points with error bars are data. The thick solid line is the best fit; the thin solid line is the total background. The thick dashed line is the fitted signal for the $\eta(1760)$. The thin dashed, dot-dashed and dotted lines are the NR, b_1 and b_2 background components, respectively.

B. Results of the $X(1835)$ fit

According to existing observations [1, 6], two resonances, $X(1835)$ and $\eta(1760)$, have been reported in the lower mass region above the $\eta'\pi^+\pi^-$ threshold. Assuming that both $X(1835)$ and $\eta(1760)$ have the same spin-parity of $J^{PC} = 0^{-+}$, the effect of interference between these two states must be taken into account in any attempt to extract a signal yield for the $X(1835)$. Each resonance is described by a BW amplitude:

$$g_{BW}(W) = \frac{1}{(W^2 - M^2) + i\Gamma M}, \tag{5}$$

and the amplitude for the two interfering resonances is written as

$$\mathcal{M}(W) = A_1 \cdot g_{BW1}(W) + A_2 \cdot g_{BW2}(W) \cdot e^{i\phi}, \tag{6}$$

where ϕ is the relative phase between the two resonances and A_1 and A_2 are normalization factors.

Under the assumption of non-interference between the R and NR components, a fit with the $X(1835)$ and $\eta(1760)$ signals plus their interference is performed to the lower-mass events. Here, the $X(1835)$ mass and width are fixed at the BES values [6]. We find two solutions with equally good fit quality and the same $\eta(1760)$ mass and width; the results are shown in Fig. 4. In either solution, the statistical significance is 2.9σ for the $X(1835)$ and 4.1σ for the $\eta(1760)$. The relative phase between the two resonances is determined to be $\phi_1 = (287^{+42}_{-51})^\circ$ for the constructive-interference solution and $\phi_2 = (139^{+19}_{-9})^\circ$ for the destructive-interference one. The signal yields for the two solutions are determined to be $Y_1 = 332^{+140}_{-122}$ and $Y_2 = 632^{+224}_{-231}$ for the $X(1835)$ and $Y_1 = 52^{+35}_{-20}$ and $Y_2 = 315^{+223}_{-165}$ for the $\eta(1760)$. The fitted mass and width of the $\eta(1760)$ are $M = (1703^{+12}_{-11})$ MeV/c^2 and $\Gamma = (42^{+36}_{-22})$ MeV/c^2. Upper

limits on the product $\Gamma_{\gamma\gamma}\mathcal{B}(\eta'\pi^+\pi^-)$ for the $X(1835)$ at the 90% confidence level are determined to be 35.6 eV/c^2 and 83 eV/c^2 for the constructive- and destructive-interference solutions, respectively. The upper limit for the signal yield at 90% confidence level is determined by integrating the likelihood distribution convolved with a Gaussian function to include the systematic error.

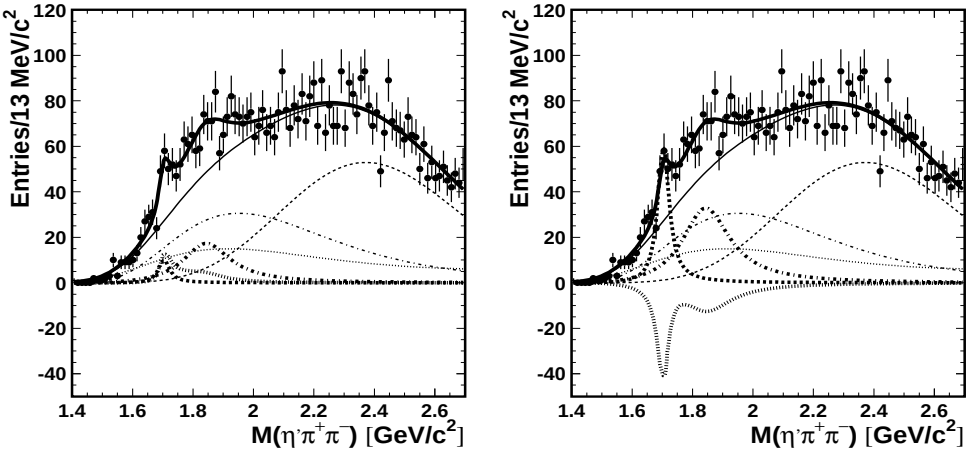

FIG. 4: Results of a combined fit for the $X(1835)$ and $\eta(1760)$ with interference between them. The points with error bars are data. The thick solid line is the fit; the thin solid line is the total background. The thick dashed (dot-dashed, dotted) line is the fitted signal for the $\eta(1760)$ ($X(1835)$, the interference term between them). The thin dashed, dot-dashed and dotted lines are the NR, b_1 and b_2 background components, respectively. The left (right) panel represents the solution with constructive (destructive) interference.

Another fit without interference between the resonances is performed to examine the significance of the $X(1835)$ signal. The statistical significance from the fit with two incoherent resonances is found to be 3.2σ for the $X(1835)$ and 4.4σ for the $\eta(1760)$. The $\eta(1760)$ mass and width are fitted to be $M = (1707.7^{+8.7}_{-7.0})$ MeV/c^2 and $\Gamma = (45^{+34}_{-21})$ MeV/c^2, respectively. The products of the two-photon decay width and the branching fraction for the $X(1835)$ and $\eta(1760)$ decays to $\eta'\pi^+\pi^-$ are estimated as $\Gamma_{\gamma\gamma}\mathcal{B}(X(1835) \to \eta'\pi^+\pi^-) = (23.1^{+6.3}_{-6.6})$ eV/c^2 and $\Gamma_{\gamma\gamma}\mathcal{B}(\eta(1760) \to \eta'\pi^+\pi^-) = (6.7^{+2.8}_{-2.3})$ eV/c^2. The inclusion of the interference only mildly improves the fit. The statistical significance of the interference term, defined as $\sqrt{-2\ln(\mathcal{L}_{\rm no}/\mathcal{L}_{\rm yes})}$, is 0.69σ, where $\mathcal{L}_{\rm yes}$ ($\mathcal{L}_{\rm no}$) is the likelihood value of the fit with (without) interference. There is a minor difference in the $\eta(1760)$ mass and width between the two fits with and without interference. The statistical significance of the $\eta(1760)$ mass difference between the fit result and the world-average value [1] is calculated as $\sqrt{-2\ln(\mathcal{L}_{\rm fixed}/\mathcal{L}_{\rm free})}$, and is found to be 2.6σ (3.1σ) for the two coherent (incoherent) resonances. Here, $\mathcal{L}_{\rm fixed}$ and $\mathcal{L}_{\rm free}$ are the likelihood values of the fits with the $\eta(1760)$ mass fixed at the world-average value and floating, respectively.

In the determination of the $X(1835)$ and $\eta(1760)$ significances, we have examined the effect of uncertainties of the following factors: (1) the $X(1835)$ mass or width varied by $\pm1\sigma$; (2) a background fluctuation by changing the fit region; (3) a background function that uses three threshold functions convolved with two-photon luminosity, efficiency and mass resolution; (4) a fluctuation in the b_1 component by moving the η'-*sdb* selection mass window; (5) a variation of $\pm1\sigma$ in each of the background function parameters for the b_1 or b_2 components. The fits of two incoherent resonances are performed under the variations listed above. The lowest (highest) significance 3.9σ (5.0σ) for the $\eta(1760)$ is obtained with the $X(1835)$ width increased (decreased) by 1σ, while the significances under the rest of variations are compatible with the values from the incoherent fit of 3.2σ for the $X(1835)$ and 4.4σ for the $\eta(1760)$. To ensure reliable estimation for the $X(1835)$, a fit with floating masses and widths for both the $X(1835)$ and the $\eta(1760)$ is performed. The yields, masses and widths are fitted to be $Y = (444 \pm 158)$, $M = (1833 \pm 30)$ MeV/c^2 and $\Gamma = (202 \pm 66)$ MeV/c^2 for the $X(1835)$ and $Y = (104 \pm 75)$, $M = (1706.9 \pm 8.3)$ MeV/c^2 and $\Gamma = (40 \pm 36)$ MeV/c^2 for the $\eta(1760)$. In all variations, the fitted parameters for the $X(1835)$ are consistent with those in the BES experiment.

C. Angular distribution

We examined the distribution of θ^*, the angle between the η' momentum and the beam direction in the $\gamma\gamma$ rest frame. The angular distribution is determined from R and NR yields extracted from fitting the $|\sum \vec{p}_t^{\,*}|$ distribution

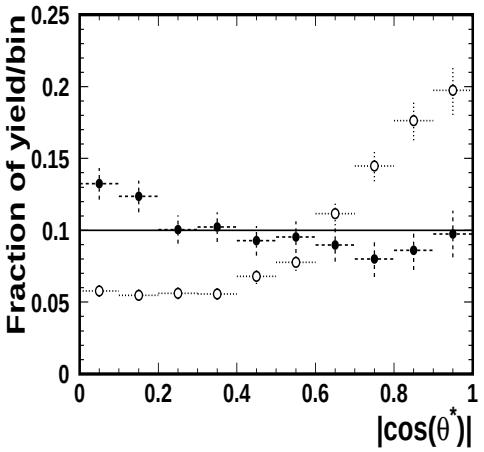

FIG. 5: Angular distributions in the $\gamma\gamma$ rest frame for two mass regions. The solid circles are for the $X(1835)$ and $\eta(1760)$ region; the open circles are for the NR component in the upper sideband region. The yield in each bin is corrected for the efficiency and normalized to the sum of the corrected yield. The horizontal line at $y = 0.1$ represents an isotropic MC distribution.

sliced into ten angular bins for the mass region of the $X(1835)$ and $\eta(1760)$ ($W < 2.04$ GeV/c^2) and its upper sideband ($W \in (2.2, 2.7)$ GeV/c^2). The distribution in the upper sideband region shows forward and backward peaks characteristic of a higher-angular-momentum component, which indicates strong contributions from the $\eta' f_2(1270)$ production (see Fig. 5). Indeed, a large $f_2(1270)$ signal is observed in the $\pi^+\pi^-$ invariant mass distribution for the $\eta'\pi^+\pi^-$ events selected in that region, as shown in Fig. 6. The dominant $\eta' f_2(1270)$ component in the upper sideband region shows interesting dynamics with a broad structure with favored quantum numbers $J^P = 2^+$. A nearly isotropic distribution in the mass region below 2.04 GeV/c^2 after the efficiency correction (with $\chi^2/N_{dof} = 9.9/9$) is compatible with the assumption of pseudoscalar quantum numbers for the $\eta(1760)$ and $X(1835)$. However, a possible non-flat distribution for the NR will influence the distribution for the R component; thus, a plausible J^P value for each R should be examined with the NR component subtracted once the existence of the $\eta(1760)$ and $X(1835)$ production is clarified. No significant intermediate state is seen in the mass region below 2.04 GeV/c^2. However, a minor contribution from another $J^P = 2^-$ resonance [30] cannot be ruled out.

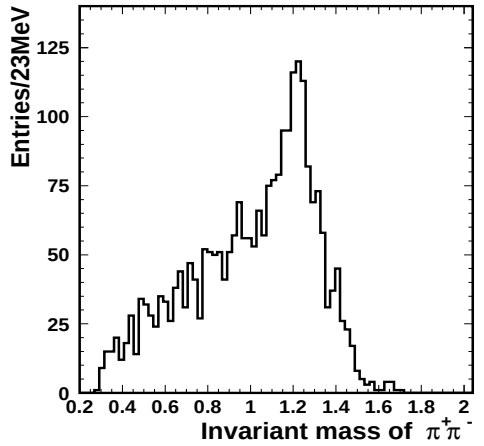

FIG. 6: Invariant mass distribution of $\pi^+\pi^-$ for the $\eta'\pi^+\pi^-$ events selected in the upper sideband region of 2.2 GeV/$c^2 < W <$ 2.7 GeV/c^2, where a large signal for $f_2(1270) \to \pi^+\pi^-$ decays is shown.

D. Results of the $\eta_c(1S)$ fit

We first assume that there is no interference between the $\eta_c(1S)$ and the NR background. Figure 7 shows the $\eta'\pi^+\pi^-$ invariant mass distribution for the candidates with mass greater than 2.6 GeV/c^2 together with the fitted

signal and background curves. The $\eta_c(1S)$ mass and width are determined to be $M = (2982.7 \pm 1.8)$ MeV/c^2 and $\Gamma = (37.8^{+5.8}_{-5.3})$ MeV/c^2. The product of the two-photon decay width and branching fraction for the $\eta_c(1S)$ is calculated using Eq. (4). Using the fitted $\eta_c(1S)$ signal yield of $n_s = 486^{+40}_{-39}$, we determine $\Gamma_{\gamma\gamma}\mathcal{B}(\eta_c(1S) \to \eta'\pi^+\pi^-) = (50.5^{+4.2}_{-4.1})$ eV/c^2.

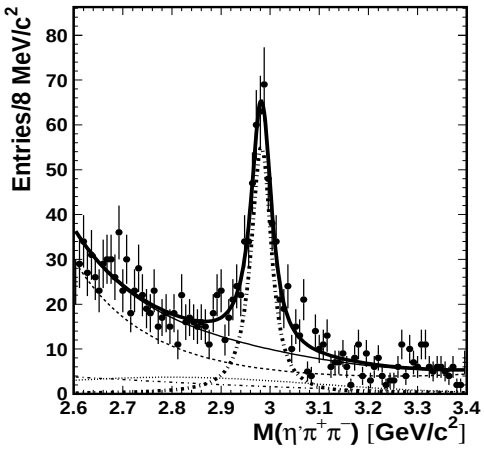

FIG. 7: The invariant mass distribution for the $\eta'\pi^+\pi^-$ candidates in the mass range above 2.6 GeV/c^2. The points with error bars are data. The thick-solid line is the fit; the thin-solid line is the total background. The thick dot-dashed line is the fitted signal for the $\eta_c(1S)$. The thin dashed, dot-dashed and dotted lines are the NR, b_1 and b_2 background components, respectively.

We now address the effect of possible interference between the $\eta_c(1S)$ resonance, hereafter referred to as R, and the non-resonant component. A precise description of the data in this case is impossible without a good understanding of the background. As discussed in section V-C, the NR component in the mass region above 2.2 GeV/c^2 has a contamination of events from non-0^- production via two-photon processes. Although contamination is evident even in the $\eta_c(1S)$ mass region, our data sample is insufficient to determine the type and rate of production of the non-0^- states in this mass region. The NR component in our analysis can be subdivided into two types: one for the non-resonant final state (denoted as $NR1$) that interferes with R and the other for production of various non-0^- states (denoted $NR2$) that do not interfere with the R. The amplitude for R production with interference with the $NR1$ term is written as

$$\mathcal{M}(W) = A \cdot g_{BW}(W) \cdot e^{i\phi} + A_{NR1} \cdot g_{NR1}(W), \tag{7}$$

where g_{BW} is the BW function in Eq. (5), g_{NR1} is assumed to be a real function for $NR1$, ϕ is the interference phase, and A and A_{NR1} are normalization factors. Assuming that $NR1$ and $NR2$ have the same shape, the fitting function in Eq. (3) for the R and NR components—where R interferes with $NR1$ but not with $NR2$—can be expressed as

$$f = n_s \cdot f_s(u; M, \Gamma) + n_{NR} \cdot f_{NR}(u; p_{NR}) + f_{int}, \tag{8}$$

where the interference term is

$$f_{int} = 2\sqrt{\alpha_{NR} \cdot n_{NR} \cdot f_{NR}(u; p_{NR})} \cdot \sqrt{n_s \cdot f_s(u; M, \Gamma)} \cdot \cos(\theta + \phi) \tag{9}$$

with $\alpha_{NR} = n_1/n_{NR}$, $n_{NR} = n_1 + n_2$, and n_1 and n_2 are the number of $NR1$ and $NR2$ events, respectively. An intrinsic phase θ is determined by the R mass, width and W value. The function f, including the f_{int} term, is convolved with a mass resolution function after corrections for $dL_{\gamma\gamma}/dW$ and efficiency. The f_s and f_{NR} PDFs are normalized; the function f_{int} is fully determined by the fit parameters.

To investigate the possible effect of interference with the NR component, a fit to the $\eta_c(1S)$ signal with interference with $NR1$ but without interference with $NR2$ is performed for various initial input values for the α_{NR} and ϕ parameters. For the $\eta_c(1S)$, the fit gives two solutions with almost the same maximum likelihood value; the mass and width of the $\eta_c(1S)$ are $M = 2982.7$ (2983.0) MeV/c^2 and $\Gamma = 36.4$ MeV/c^2 at $\alpha_{NR} = 0.01\%$ (100%); these are quite consistent with the result of the fit without interference. The differences in the $\eta_c(1S)$ mass and width with and without interference, $\Delta M = 0.3$ MeV/c^2 and $\Delta\Gamma = 1.4$ MeV/c^2, are taken as model-dependent uncertainties in the determination of the mass and width. However, the fits give very different values for the $\eta_c(1S)$ yield. If, for example, α_{NR} is fixed at 100% in the fit with interference, the yields obtained are $Y_1 = 854 \pm 59$ with $\phi_1 = (-92 \pm 5)^\circ$ for

destructive interference and $Y_2 = 264 \pm 22$ with $\phi_2 = (91 \pm 8)^\circ$ for constructive interference, while the $\eta_c(1S)$ yield of the incoherent fit is 486^{+40}_{-39}. A strong correlation between α_{NR} and ϕ is observed from the fits: ϕ_1 and ϕ_2 are close to 180° and -180° (90° and -90°), respectively, if α_{NR} is close to zero (100%). The insensitivity of the maximum likelihood value for the fits in the full α_{NR} region between zero and 100% and a strong correlation between α_{NR} and ϕ imply large uncertainties in the determination of α_{NR}, ϕ and the strength of the interference term. With an additional error source from the interference term, the $\eta_c(1S)$ yield has also a large uncertainty ranging from 264 ± 22 to 486 ± 40 for constructive interference and from 486 ± 40 to 854 ± 59 for destructive interference depending on the true α_{NR} and ϕ values. Our fit results, as well as the absence of any visual asymmetry in the $\eta_c(1S)$ line shape in the data, indicate that the interference term cannot be determined without independent information on the $NR1$ component such as its angular distribution in the $\eta_c(1S)$ sideband mass region. The measured mass and width of the $\eta_c(1S)$ have a marginal dependence on the interference, while the yield is strongly correlated with the interference component and, thus, cannot be determined precisely with the existing data sample. The situation would improve if the interference effect were determined independently with a much larger data sample.

VI. SYSTEMATIC ERRORS

To examine a possible bias in the mass measurement for the decay $R \to \eta'\pi^+\pi^-$, a data sample of $D^0 \to \eta' K^0_S$ decays with $K^0_S \to \pi^+\pi^-$ is selected with tight mass window requirements for the η and η'. The D^0 mass resulting from a fit of the invariant mass spectrum of $\eta' K^0_S$ is lower than its nominal value by 1.4 MeV/c^2, which is taken as an uncertainty of the mass scale after a linear correction for mass value. The uncertainty in the width determination can arise from a difference in the mass resolution between data and MC simulation. This is estimated by changing the mass resolution by ± 1 MeV/c^2 and is found to be 2.0 MeV/c^2 for the $\eta_c(1S)$ and 10 MeV/c^2 for the $\eta(1760)$. Systematic errors on the mass, width and $\Gamma_{\gamma\gamma}\mathcal{B}$ product due to uncertainties in the NR background estimation are determined by varying the fit mass interval and $|\sum \vec{p}^*_t|$ requirement separately. The error contributions from uncertainties in determination of the b_1 and b_2 backgrounds are minor for the $\eta_c(1S)$ but are sizable in the mass region below 2 GeV/c^2. The uncertainties in the resonance parameters, estimated by varying the shape parameters and yields of the b_1 and b_2 backgrounds by $\pm 1\sigma$ and added in quadrature, are taken as the corresponding errors for the $X(1835)$ and $\eta(1760)$, respectively.

There are additional sources of systematic errors in the $\Gamma_{\gamma\gamma}\mathcal{B}$ product determination. The trigger efficiency for four-track events is relatively high because of redundant two-track and multi-track triggers in the Belle first-level trigger. From the trigger simulation program, the difference in the efficiency with and without both trigger conditions satisfied is found to be 1% (2.7%) at an invariant mass of 2.98 (1.84) GeV/c^2; this is included as a systematic error. The efficiency for the pion identification, determined by using the inclusive D^* sample, is lower than that from MC simulation by (1.40 ± 0.64)% for the $\eta_c(1S)$ and (0.02 ± 0.60)% for the $\eta(1760)$, and the corresponding contributions to the systematic error are 1.5% and 0.6%, respectively. The reconstruction efficiency for $\eta \to \gamma\gamma$ is studied with an inclusive η sample, and its deviation from the MC simulation plus its error in quadrature is 4.9%. The uncertainty in the track reconstruction efficiency is 5.5% and that of the π^0-veto requirement is 3%. The accuracy of the two-photon luminosity function calculated by the TREPS generator is estimated to be about 5% including the error from neglecting radiative corrections (2%), the uncertainty from the form factor effect (2%), and the error of the total integrated luminosity (1.4%) [23]. The background contribution from the initial-state radiation processes is negligible [2]. Furthermore, the run-dependent background conditions add an additional uncertainty of 3% in the yield determination. A dominant source of systematic errors for the $X(1835)$ yield is the uncertainty of its decay width. It is estimated to be 18% by changing the width by $\pm 1\sigma_\Gamma$ in the fit for the yield extraction.

The systematic errors in the measurements of the mass and width for the $\eta_c(1S)$ and $\eta(1760)$, as well as of the product $\Gamma_{\gamma\gamma}\mathcal{B}$ for each resonance, are summarized in Table I.

VII. RESULTS AND DISCUSSION

The results for the yields, masses and widths, as well as the product decay widths are summarized in Table II for the $\eta_c(1S)$ and in Table III for the $\eta(1760)$ and $X(1835)$.

The $\eta_c(1S)$ mass and width are measured to be $M = (2982.7 \pm 1.8(stat) \pm 2.2(syst) \pm 0.3(model))$ MeV/c^2 and $\Gamma = (37.8^{+5.8}_{-5.3}(stat) \pm 2.8(syst) \pm 1.4(model))$ MeV/c^2, and are consistent with the recent results from BES [3] and Belle [5]. If we assume that there is no interference, the directly measured product for the $\eta_c(1S)$ decay width to $\eta'\pi^+\pi^-$ is determined to be $\Gamma_{\gamma\gamma}\mathcal{B}(\eta_c(1S) \to \eta'\pi^+\pi^-) = (50.5^{+4.2}_{-4.1} \pm 5.6)$ eV/c^2, which is marginally consistent with the existing value (194 ± 97) eV/c^2 from the indirect measurements [1]. Instead of a direct reference to the world-average value for $\Gamma_{\gamma\gamma}(\eta_c(1S))$, we determine it from the ratio of $\Gamma_{\gamma\gamma}\Gamma(K\overline{K}\pi)/\Gamma_{\rm total} = (0.407 \pm 0.027)$ keV/c^2 to

TABLE I: Summary of systematic uncertainty contributions to the mass and width for the $\eta_c(1S)$ and $\eta(1760)$ and to $\Gamma_{\gamma\gamma}\mathcal{B}$ for the $\eta_c(1S)$, $\eta(1760)$ and $X(1835)$. 1-R and 2-R denote one and two resonances in the fit, respectively.

Source	$\eta_c(1S)$	$\eta(1760)$		$X(1835)$
	1-R fit		2-R fit	
$\triangle(M)$ (MeV/c^2)				
Mass scale	2.2	1.3		-
Background shape	0.1	8	0.5	-
η' sideband and b_{any}	0.0	3.9	0.2	-
$\lvert\sum\vec{p}_t^{\,*}\rvert$ requirement	0.4	4.5	0.6	-
$X(1835)$ Width	-	-	0.9	-
Total	2.2	10	1.8	-
$\triangle(\Gamma)$ (MeV/c^2)				
Mass resolution	2.0	10	1.5	-
Background shape	1.9	7	6	-
η' sideband and b_{any}	0.02	17	7.1	-
$\lvert\sum\vec{p}_t^{\,*}\rvert$ requirement	0.4	14	9	-
$X(1835)$ Width	-	-	8	-
Total	2.8	25	15	-
$\triangle(\Gamma_{\gamma\gamma}\mathcal{B})/(\Gamma_{\gamma\gamma}\mathcal{B})$ (%)				
$X(1835)$ Width	-	-	16	18
Background shape	4.6	2	13	2.6
η' sideband and b_{any}	0.03	7.3	15	3.8
$\lvert\sum\vec{p}_t^{\,*}\rvert$ requirement	2.2	0.6	6.9	6.3
Trigger efficiency	1		2.7	
π ID efficiency	1.5		0.6	
η rec. efficiency			4.9	
Track rec. efficiency			5.5	
π^0 veto			3	
Two-photon Luminosity			5	
Run dependence			3	
Total	11	13	28	22

TABLE II: Summary of the results for the $\eta_c(1S)$: M and Γ are the mass and width; Y is the yield; $\mathcal{B}$ is the branching fraction for $\eta_c(1S) \to \eta'\pi^+\pi^-$; $\Gamma_{\gamma\gamma}\mathcal{B}$ is the product of the two-photon decay width and the branching fraction. The world-average values are shown for comparison.

Parameters	This work	PDG
Y	$486^{+40}_{-39} \pm 53$	
M, MeV/c^2	$2982.7 \pm 1.8 \pm 2.2$	2980.3 ± 1.2
Γ, MeV/c^2	$37.8^{+5.8}_{-5.3} \pm 2.8$	26.7 ± 3
$\Gamma_{\gamma\gamma}\mathcal{B}$, eV/$c^2$	$50.5^{+4.2}_{-4.1} \pm 5.6$	194 ± 97
$\mathcal{B}$, %	0.87 ± 0.20	2.7 ± 1.1

$\Gamma(K\overline{K}\pi)/\Gamma_{\rm total} = (7.0 \pm 1.2) \times 10^{-2}$ [1], and obtain the width $\Gamma_{\gamma\gamma}(\eta_c(1S)) = (5.8 \pm 1.1)$ keV/c^2 with a smaller relative error. With that as an input, the branching fraction is calculated to be $\mathcal{B}(\eta_c(1S) \to \eta'\pi^+\pi^-) = (0.87 \pm 0.20)\%$, where both statistical and systematic errors are included.

We report the first evidence for $\eta(1760)$ decay to $\eta'\pi^+\pi^-$ and find two solutions for its parameters, depending on the inclusion or not of the $X(1835)$, whose existence is marginal in our fits. The decay $\eta(1760) \to \eta'\pi^+\pi^-$ is found with a significance of 4.7σ including systematic error, with the assumption that the $X(1835)$ is not produced; the $\eta(1760)$ mass and width are determined to be $M = (1768^{+24}_{-25} \pm 10)$ MeV/c^2 and $\Gamma = (224^{+62}_{-56} \pm 25)$ MeV/c^2. The fitted $\eta(1760)$ mass is consistent with the existing measurements [17, 18]. The product of the two-photon decay width and the branching fraction for the $\eta(1760)$ decay to $\eta'\pi^+\pi^-$ is determined to be $\Gamma_{\gamma\gamma}\mathcal{B}(\eta(1760) \to \eta'\pi^+\pi^-) = (28.2^{+7.9}_{-7.5} \pm 3.7)$ eV/c^2. When the mass spectrum is fitted with two coherent resonances, the $\eta(1760)$ and $X(1835)$, the $\eta(1760)$ mass and width are found to be $M = (1703^{+12}_{-11} \pm 1.8)$ MeV/c^2 and $\Gamma = (42^{+36}_{-22} \pm 15)$ MeV /c^2, and the signal significances including the systematic error estimated to be 4.1σ for the $\eta(1760)$ and 2.8σ for the $X(1835)$. Upper

TABLE III: Summary of the results for $\eta(1760)$ and $X(1835)$: M and Γ are the mass and width; Y is the yield; $\Gamma_{\gamma\gamma}\mathcal{B}$ is the product of the two-photon decay width and branching fraction; Y_{90} and $(\Gamma_{\gamma\gamma}\mathcal{B})_{90}$ are the upper limits at 90% confidence level with systematic error included. The $\eta(1760)$ mass and width from the two-resonance fit with interference, as well as world average values, are shown for comparison. S is the signal significance including systematic errors.

Parameter	One resonance	Two interfering resonances		Reference
		Solution I	Solution II	
		$X(1835)$		
M, MeV/c^2		1836.5 (fixed)		$1836.5 \pm 3.0^{+5.6}_{-2.1}$ [6]
Γ, MeV/c^2		190 (fixed)		$190 \pm 9^{+38}_{-36}$ [6]
Y		$332^{+140}_{-122} \pm 73$	$632^{+224}_{-231} \pm 139$	
Y_{90}		< 650	< 1490	
$\Gamma_{\gamma\gamma}\mathcal{B}$, eV/$c^2$		$18.2^{+7.7}_{-6.7} \pm 4.0$	$35^{+12}_{-13} \pm 8$	
$(\Gamma_{\gamma\gamma}\mathcal{B})_{90}$ eV/c^2		< 35.6	< 83	
S, σ		2.8		
		$\eta(1760)$		
M, MeV/c^2	$1768^{+24}_{-25} \pm 10$	$1703^{+12}_{-11} \pm 1.8$		1756 ± 9 [1]
Γ, MeV/c^2	$224^{+62}_{-56} \pm 25$	$42^{+36}_{-22} \pm 15$		96 ± 70 [1]
Y	$465^{+131}_{-124} \pm 60$	$52^{+35}_{-20} \pm 15$	$315^{+223}_{-165} \pm 88$	
$\Gamma_{\gamma\gamma}\mathcal{B}$, eV/$c^2$	$28.2^{+7.9}_{-7.5} \pm 3.7$	$3.0^{+2.0}_{-1.2} \pm 0.8$	$18^{+13}_{-10} \pm 5$	
S, σ	4.7	4.1		
ϕ		$(287^{+42}_{-51})^\circ$	$(139^{+19}_{-9})^\circ$	

limits on the product $\Gamma_{\gamma\gamma}\mathcal{B}$ for the $X(1835)$ decay to $\eta'\pi^+\pi^-$ at the 90% confidence level for two fit solutions are determined: $\Gamma_{\gamma\gamma}\mathcal{B}(X(1835) \to \eta'\pi^+\pi^-) < 35.6$ eV/c^2 with $\phi_1 = (287^{+42}_{-51})^\circ$ for constructive interference and $\Gamma_{\gamma\gamma}\mathcal{B}(X(1835) \to \eta'\pi^+\pi^-) < 83$ eV/c^2 with $\phi_2 = (139^{+19}_{-9})^\circ$ for destructive interference.

In summary, we report the first observation of $\eta'\pi^+\pi^-$ production in two-photon collisions. We measure the mass, width and the product of the two-photon width and the branching fraction for the η_c. We also report the first evidence for the $\eta'\pi^+\pi^-$ decay mode of the $\eta(1760)$. No strong evidence for the $X(1835)$ is found.

Acknowledgments

We extend our special thanks to J.X. Wang of IHEP (Beijing) for many helpful discussions. We thank the KEKB group for the excellent operation of the accelerator; the KEK cryogenics group for the efficient operation of the solenoid; and the KEK computer group, the National Institute of Informatics, and the PNNL/EMSL computing group for valuable computing and SINET4 network support. We acknowledge support from the Ministry of Education, Culture, Sports, Science, and Technology (MEXT) of Japan, the Japan Society for the Promotion of Science (JSPS), and the Tau-Lepton Physics Research Center of Nagoya University; the Australian Research Council and the Australian Department of Industry, Innovation, Science and Research; the National Natural Science Foundation of China under contract No. 10575109, 10775142, 10875115 and 10825524; the Ministry of Education, Youth and Sports of the Czech Republic under contract No. LA10033 and MSM0021620859; the Department of Science and Technology of India; the Istituto Nazionale di Fisica Nucleare of Italy; the BK21 and WCU program of the Ministry Education Science and Technology, National Research Foundation of Korea, and GSDC of the Korea Institute of Science and Technology Information; the Polish Ministry of Science and Higher Education; the Ministry of Education and Science of the Russian Federation and the Russian Federal Agency for Atomic Energy; the Slovenian Research Agency; the Swiss National Science Foundation; the National Science Council and the Ministry of Education of Taiwan; and the U.S. Department of Energy and the National Science Foundation. This work is supported by a Grant-in-Aid from MEXT for Science Research in a Priority Area ("New Development of Flavor Physics"), and from JSPS for Creative Scientific Research ("Evolution of Tau-lepton Physics").

[1] K. Nakamura *et al.* (Particle Data Group), J. Phys. G **37**, 075021 (2010).
[2] S. Uehara *et al.* (Belle Collaboration), Eur. Phys. J. C **53**, 1 (2008).

[3] M. Ablikim *et al.* (BESIII Collaboration), Phys. Rev. Lett. **108**, 222002 (2012).
[4] N. Brambilla *et al.*, Eur. Phys. J. C **71**, 1534 (2011).
[5] A. Vinokurova *et al.* (Belle Collaboration), Phys. Lett. B **706**, 139 (2011).
[6] M. Ablikim *et al.* (BESIII Collaboration), Phys. Rev. Lett. **106**, 072002 (2011); M. Ablikim *et al.* (BES Collaboration), Phys. Rev. Lett. **95**, 262001 (2005).
[7] S.L. Zhu and C.S. Gao, Commun. Theor. Phys. **46**, 291 (2006); Z.G. Wang and S.L. Wan, J. Phys. G **34**, 505 (2007).
[8] G.J. Ding and M.L. Yan, Eur. Phys. J. A **28**, 351 (2006).
[9] N. Kochelev and D.P. Min, Phys. Rev. D **72**, 097502 (2005); Phys. Lett. B **633**, 283 (2006).
[10] B.A. Li, Phys. Rev. D **74**, 034019 (2006).
[11] X.G. He, X.Q. Li, X. Li and J.P. Ma, Eur. Phys. J. C **49**, 731 (2007).
[12] T. Huang and S.L. Zhu, Phys. Rev. D **73**, 014023 (2006).
[13] E. Klempt and A. Zaitsev, Phys. Rept. **454**, 1 (2007).
[14] J.Z. Bai *et al.* (BES Collaboration), Phys. Rev. Lett. **91**, 022001 (2003).
[15] M. Ablikim *et al.* (BESIII Collaboration), Chin. Phys. C **34**, 421 (2010).
[16] R.M. Baltrusaitis *et al.* (MARKIII Collaboration), Phys. Rev. Lett. **55**, 1723 (1985); Phys. Rev. D **33**, 1222 (1986).
[17] D. Bisello *et al.* (DM2 Collaboration), Phys. Rev. D **39**, 701 (1989); Phys. Lett. B **192**, 239 (1987).
[18] M. Ablikim *et al.* (BES Collaboration), Phys. Rev. D **73**, 112007 (2006); J.Z. Bai *et al.* (BES Collaboration), Phys. Lett. B **446**, 356 (1999).
[19] P.R. Page and X.Q. Li, Eur. Phys. J. C **1**, 579 (1998).
[20] J.L. Rosner, AIP Conf. Proc. **815**, 218 (2006).
[21] A. Abashian *et al.* (Belle Collaboration), Nucl. Instrum. Methods Phys. Res., Sect. A **479**, 117 (2002).
[22] S. Kurokawa and E. Kikutani, Nucl. Instrum. Methods Phys. Res. Sect. A **499**, 1 (2003), and other papers included in this volume.
[23] S. Uehara, KEK Report 96-11 (1996).
[24] V.M. Budnev, I.F. Ginzburg, G.V. Meledin and V.G. Serbo, Phys. Rep. C **15**, 181 (1975); J. Field, Nucl. Phys. B **168**, 477 (1980), and Erratum-ibid, B **176**, 545 (1980).
[25] T. Sjöstrand, Comput. Phys. Commun. **82**, 74 (1994).
[26] The detector response is simulated with GEANT, R. Brun *et al.*, GEANT 3.21, CERN Report DD/EE/84-1, 1984.
[27] S. Uehara *et al.* (Belle Collaboration), Phys. Rev. D **82**, 114031 (2010).
[28] H. Nakazawa (Belle Collaboration), Nucl. Phys. Proc. Suppl. **124**, 220 (2008).
[29] I.C. Brock, A Fitting and Plotting Package Using MINUIT, version 4.07, Dec. 22th, 2000. The threshold function in MINUIT is defined as $f_{thresh}(x) = A \cdot (x - x_0)^p e^{c_1(x-x_0)+c_2(x-x_0)^2}$, where A, p, c_1, c_2 and x_0 are parameters.
[30] K. Karch *et al.* (Crystal Ball Collaboration), Z. Phys. C **54**, 33 (1992).